RSC Advances

PAPER

View Article Online
View Journal | View Issue

Cite this: *RSC Adv.*, 2025, **15**, 17706

Synthesis of an amphiphilic bi-prodrug based on gossypol and cytarabine for drug self-delivery†

Jianzhong Li,‡[ab] Qiang Wang,‡[a] Xinping Liu,[a] Hailong Liu,[a] Ling-na Han*[c] and Xiao Duan *[a]

Received 12th April 2025
Accepted 14th May 2025

DOI: 10.1039/d5ra02555a

rsc.li/rsc-advances

Drug–drug conjugates have become a research hotspot in nanomedicine. An amphiphilic assembled drug–drug conjugate can achieve drug self-delivery without any carriers and change the distribution of free drugs. Herein, we synthesized a pH-responsive bi-prodrug of gossypol (**GP**) and cytarabine (**Ara-C**) for cancer therapy. FT-IR, UV-vis, TLC and MS confirmed that **GP-Ara-C** was successfully synthesized. The nanoparticle size of **GP-Ara-C** is approximately 100 nm, and the stability of **GP-Ara-C** is maintained for 6 days in pH 7.4 phosphate-buffered saline (PBS). HeLa cell viability results showed that **GP-Ara-C** exhibited anticancer ability similar to that of free **GP**. Cellular uptake demonstrated that **GP-Ara-C** could be distributed in cell nuclei at 7 h. Altogether, this amphiphilic **GP-Ara-C** could be assembled into nanomedicine in an aqueous environment and could be a candidate for cancer therapy in clinics.

Introduction

Combination chemotherapy is the common method for treating cancer in human beings.[1] It can achieve synergistic effects, increase the therapeutic index, decrease single drug dose with fewer side effects and prevent drug resistance.[2,3] However, it cannot change the kinetic parameters of a single drug and simultaneously distribute two drugs into tumor tissues *in vivo*.[3,4] Using amphiphilic bi-prodrugs could be an alternative method for addressing the drawbacks of combination chemotherapy. Thus far, a few drug–drug conjugates[5–11] have been synthesized and used for cancer therapy. For example, Yan and co-workers synthesized an amphiphilic drug–drug conjugate based on the hydrophilic drug irinotecan and the hydrophobic drug chlorambucil to achieve higher anticancer activity. This conjugate could be assembled into a nanoparticle and showed a longer half-life and higher distribution in tumor tissues compared with a single drug.[12] Construction of assembled drug–drug conjugates in an aqueous environment should involve careful selection of hydrophobic and hydrophilic single drugs. Ni and co-workers selected the stronger hydrophilic drug gemcitabine compared with other anticancer drugs to prepare a glutathione-responsive camptothecin-ss-1,2,3-triazole-gemcitabine conjugate for combination chemotherapy.[13] To endow the amphiphilic drug–drug conjugates with targeting ability, the superstrong hydrophilic molecule of lactose with hepatocyte-targeting ability was conjugated with the hydrophobic drug doxorubicin *via* a pH-responsive hydrazone bond to treat tumors.[14] Based on these drug–drug conjugates, we found that hydrophobic and hydrophilic drugs are crucial factors for constructing assembled nanomedicine.

Herein, we selected the hydrophobic drug gossypol (**GP**) and the hydrophilic drug cytarabine (**Ara-C**) to prepare amphiphilic **GP-Ara-C** nanomedicine for combination chemotherapy. **GP** is a natural molecule obtained from cottonseed and has been used as a potent antifertility drug in China. Meanwhile, the antiproliferative activities of **GP** have been investigated in cancers such as breast, colon, pancreatic, ovarian, and prostate cancer.[15,16] Moreover, it exhibits an antiproliferative effect *via* many mechanisms, such as cell cycle arrest at the G0/G1 phase,[17] inhibition of DNA polymerase alpha and topoisomerasell,[18] dual-targeting mouse double minute 2 (MDM2) and vascular endothelial growth factor (VEGF),[19] and inhibition of Bcl family proteins.[20] The hydrophilic drug **Ara-C** is a nucleoside analog approved by the Food and Drug Administration in 1969.[21] Its active form—cytarabine triphosphate (Ara-CTP)—is incorporated into DNA and induces single-strand breaks, leading to cell death.[22] Based on the different mechanisms of GP and **Ara-C** for cancer therapy, this amphiphilic **GP-Ara-C** conjugate shows synergistic anticancer ability. Moreover, the pH-responsive imine bond in the **GP-Ara-C** conjugate reacted with the aldehyde group in **GP**, and the amino group in **Ara-C** was controllably broken in the acidic tumor microenvironment. Then, two free anticancer drugs were simultaneously released into the tumor tissue to achieve authentic combination chemotherapy.

[a]*Changzhi Key Laboratory of Drug Molecular Design and Innovative Pharmaceutics, Shanxi Provincial Department-Municipal Key Laboratory Cultivation Base for Quality Enhancement and Utilization of Shangdang Chinese Medicinal Materials, School of Pharmacy, Changzhi Medical College, Changzhi 046000, China. E-mail: duanxiao0211@czmc.edu.cn; hanlingna@czmc.edu.cn*

[b]*Department of Human Anatomy, Changzhi Medical College, Changzhi 046000, China*

[c]*Department of Physiology, Changzhi Medical College, Changzhi 046000, China*

† Electronic supplementary information (ESI) available. See DOI: https://doi.org/10.1039/d5ra02555a

‡ These authors contributed equally to this work.

Experimental

Materials and instruments

Cytarabine hydrochloride (purity: 99%) was purchased from Bidepharm Biocompany (Shanghai, China). Acetate gossypol (purity: 98%) was purchased from Huateng Pharma Company. (Hunan, China). Fetal bovine serum (FBS), DID (fluorescent probe), trypsin, cell counting kit-8, culture media, other bio-agents and consumables were supplied by Beyotime company (Jiangsu, China). All other organic solvents and common consumables were purchased from Jinbaiao Biotechnology Company (Changzhi, China).

The structure of **GP-Ara-C** was characterized by Fourier Transform Infrared Spectrometer (FT-IR, Tensor 27, Bruker, Germany), Ultraviolet-visible Spectroscopy (UV-vis, TU-1901, Puxi company, Beijing, China) and Thermo Scientific Hybrid Quadrupole-Orbitrap Mass Spectrometers (Thermo, America). The purity of **GP-Ara-C** was confirmed by High Performance Liquid Chromatography (HPLC, Thermo Fisher/UltiMate 3000, Flow rate: 1 mL min^{-1}, and Mobile phase: methanol/water = 80 : 20). The particle size was measured by applying dynamic light scattering (Zetasizer Nano ZSE, Malvern) and a Transmission Electron Microscope (TEM, FEI Tecnai F30, America). Cell viability was evaluated by applying a Microplate Reader (Infinite 200Pro, TECAN), and the distribution of **GP-Ara-C** in cells was monitored using a Confocal Laser Scanning Microscope (LEICA/SP8, Germany).

Synthesis of amphiphilic GP-Ara-C

Acetate gossypol (0.2 mmol, 116 mg) and cytarabine hydrochloride (0.2 mmol, 56 mg) were added to a flask with 20 mL of anhydrous acetone. Then, a molecular sieve and stirrer were added to the flask. The flask was placed into a 50 °C water bath to react for 48 h. The reaction solution was centrifuged to obtain the supernatant. Then, the supernatant was concentrated by applying a rotary evaporator. The concentrated supernatant was purified using a silica gel column. ($V_{dichloromethane}$: $V_{tetrahydrofuran}$ = 50 : 1) (Yield: 20%).

Characterization of amphiphilic GP-Ara-C

The pure amphiphilic bi-prodrug of gossypol-cytarabine conjugate was characterized by thin-layer chromatography (TLC), HPLC, FT-IR, UV-vis and MS. The free **GP**, free **Ara-C** and **GP-Ara-C** conjugate were monitored by TLC during reaction in 48 h. A new dot (R_f = 0.6) appeared on the TLC. Afterward, the powder of free **GP**, free **Ara-C** and **GP-Ara-C** was mixed with KBr to obtain the FT-IR spectra. Meanwhile, the UV-vis spectra were measured in acetone. Finally, the MS results of **GP-Ara-C** were obtained using a quadrupole-Orbitrap mass spectrometer.

Nanoparticle size of GP-Ara-C and its stability

The **GP-Ara-C** conjugate was dissolved in pH 7.4 phosphate-buffered saline (PBS). Then, the nanoparticle size of **GP-Ara-C** was measured using DLS and TEM. Meanwhile, **GP-Ara-C** was dissolved in pH 6.0 and pH 7.4 PBS. Afterward, the stability of **GP-Ara-C** was evaluated using DLS at different times.

Cell viability assays

The HeLa cell suspension was seeded into a 96-well plate for 12 h (8000 cells per well). Then, free **GP** and **GP-Ara-C** in cultural media with different concentrations (5 μg mL^{-1}, 15 μg mL^{-1}, 30 μg mL^{-1}, 50 μg mL^{-1}, 100 μg mL^{-1}) were replaced with the old media in a 96-well plate. Afterward, CCK-8 solution (20 μL) was added into a 96-well plate at 24 h. One hour later, the 96-well plate was measured under a microplate reader at 450 nm. Finally, the cell morphology of the HeLa cells treated with free **GP** and **GP-Ara-C** was observed under a microscope.

Cellular uptake

The HeLa cell was seeded into confocal dishes for 12 h. Then, free DID and DID encapsulated **GP-Ara-C** with culture media were placed into confocal dishes. Eventually, the images at 1 h, 3 h and 7 h were captured using a confocal laser scanning microscope.

Preparation of DID@**GP-Ara-C**: DID and **GP-Ara-C** were simultaneously dissolved in DMSO. Then, the DMSO solution was dripped into PBS to obtain the solution of DID@**GP-Ara-C**. Finally, the DID@**GP-Ara-C** solution was diluted in the culture media for cellular uptake experiments.

Results and discussion

Synthesis of the GP-Ara-C conjugate

The product of **GP-Ara-C** is difficult to obtain because **GP** and **Ara-C** cannot simultaneously dissolve in $CHCl_3$, which does not trigger the aldehyde-lactol tautomerization of **GP**.[23] Moreover, we found that **GP-Ara-C** could not be obtained in DMSO. We speculated that **GP** and **Ara-C** could dissolve in DMSO simultaneously and that **GP-Ara-C** was saturated in DMSO with 17% aldehyde groups in **GP**. Studies confirmed that the characteristic proton peak of the 100% aldehyde group in **GP** appears in $CDCl_3$, 53% in CD_3OD and 17% in DMSO-d_6.[24] Furthermore, the tautomerization rate changes over time.[25] Unfortunately, **Ara-C** could not dissolve in $CHCl_3$. Therefore, the reactions of **GP** and **Ara-C** cannot be easily carried out in $CDCl_3$. We chose acetone as the solvent to conduct the reaction because it does not affect the aldehyde group during the reaction.[26] The **GP** can dissolve in acetone, and **Ara-C** only slightly dissolves in acetone. Consequently, the yield and reaction velocity were limited. Finally, a small amount of **GP-Ara-C** was synthesized by the reaction of the aldehyde group in **GP** and the amino group in **Ara-C**. The reaction mechanism of the imine bond in **GP-Ara-C** has been explained by previous researchers.[27]

Characterization of the GP-Ara-C conjugate

The structure of **GP-Ara-C** is shown in Fig. 1A. The synthesis result of **GP-Ara-C** was confirmed by TLC, HPLC, FT-IR, UV-vis and MS. We clearly observed a new dot (**GP-Ara-C**) in the TLC image (Fig. 1C). Furthermore, the FT-IR spectra (Fig. 2) showed that the characteristic peaks of new bond (–C=N–, 1629 cm^{-1})

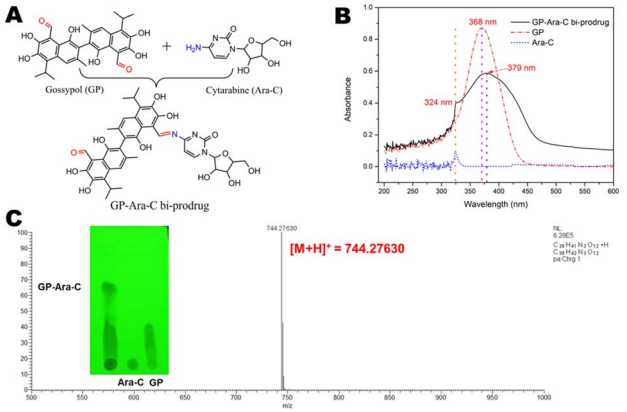

Fig. 1 (A) Structure of **GP-Ara-C**, (B) UV-vis curves of GP, Ara-C and **GP-Ara-C** in acetone, and (C) TLC and mass spectrum of **GP-Ara-C**.

in **GP-Ara-C**, alkyl (–CH_2– and –CH_3), hydroxyl (1271 cm^{-1}) and Ph–OH (1286 cm^{-1} and 1269 cm^{-1}) appeared in the spectrum of **GP-Ara-C**. Moreover, we discovered that the characteristic peaks (324 nm and 368 nm) of **Ara-C** and **GP** in acetone were simultaneously observed in the product of **GP-Ara-C** in the UV-vis curve; meanwhile, the largest absorbance peak in **GP** at 368 nm was shifted toward 379 nm in **GP-Ara-C** (Fig. 1B). Based on the most important MS results, we found that the $[M + H]^+$ ion is at m/z 744.2763. The molecular formula of **GP-Ara-C** is $C_{39}H_{41}N_3O_{12}$ (MW = 743.756), which is consistent with the MS results. These results confirmed that **GP-Ara-C** was successfully synthesized. To further confirm the structure of **GP-Ara-C** from the NMR data, we measured the NMR spectra of **GP** and **Ara-C** as control spectra. From the NMR data of **GP** in DMSO-d_6, we observe that there are no peaks in the range of 5.5–6.5 ppm. Interestingly, we observe new peaks in the range of 5.5–6.5 ppm in DMSO-d_6 in the structure of **GP-Ara-C**. This means that the new peaks in the range of 5.5–6.5 ppm in **GP-Ara-C** come from **Ara-C** (Fig. S1†). More importantly, the ^{1}H NMR, ^{13}C NMR and C–H COSY spectra of **GP-Ara-C** in $CDCl_3$ in Fig. S2† showed that the integrals of characteristic peaks (n and a positions) are 0.95 and 1.05, respectively. Combining the MS result (m/z = 744.27630) with the ratio (1 : 1) of the n position (means **GP**) and a position (means **Ara-C**), we conclude that one molecule **GP** was conjugated with one molecule **Ara-C**. Additionally, the elution times of **GP**, **Ara-C** and **GP-Ara-C** measured by HPLC showed that the product of **GP-Ara-C** was successfully purified by silica gel column (Fig. S3†).

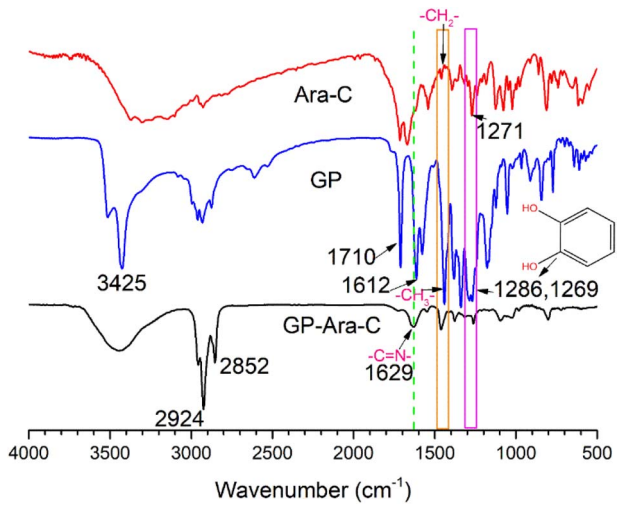

Fig. 2 IR spectra of **Ara-C**, **GP** and **GP-Ara-C**.

Nanoparticle size of GP-Ara-C and its stability

Assembled **GP-Ara-C** was measured using TEM and DLS. The TEM image showed that the assembled nanoparticle of **GP-Ara-C** (1 mg mL^{-1}) is around 30 nm derived from a dried state with significant shrinkage compared with a hydrodynamic size (Fig. 3A). When **GP-Ara-C** was dissolved in pure water, we observed a distinguishable red-light beam (Fig. 3B). Moreover, the DLS results showed that the assembled nanoparticle of **GP-Ara-C** (1 mg mL^{-1}) was around 100 nm with the hydrodynamic size (Fig. 3B) and stable for 6 days in pH 7.4 PBS (Fig. 3C). The same assembled nanoparticle of **GP-Ara-C** was quickly disrupted in hours in pH 6.0 PBS (Fig. 3D). These results confirmed that the pH-responsive bond of imine in **GP-Ara-C** was easily broken down in pH 6.0 PBS compared with pH 7.4 PBS, resulting in the disruption of nanoparticles, which could achieve the controllable disruption of assembled nanoparticles in the acidic microenvironment in tumor tissues.

Cell viability assays

The HeLa cell viability of **GP-Ara-C** was evaluated using CCK-8 assays. The IC_{50} values of free acetate **GP** and **GP-Ara-C** were 50 μg mL^{-1} and 70 μg mL^{-1} at 24 h, respectively. Meanwhile, we observe cell proliferation at different concentrations of free acetate **GP** and **GP-Ara-C**. As depicted in Fig. 4, the cell proliferation was significantly inhibited at the concentration of acetate **GP** 50 μg mL^{-1}, and the drug efficacy of **GP-Ara-C** was similar to that of acetate **GP** for HeLa cells, demonstrating that the modification with **Ara-C** by imine bond could not affect the anticancer ability of acetate **GP**. To obtain observable images of HeLa cell morphology, we particularly captured images of

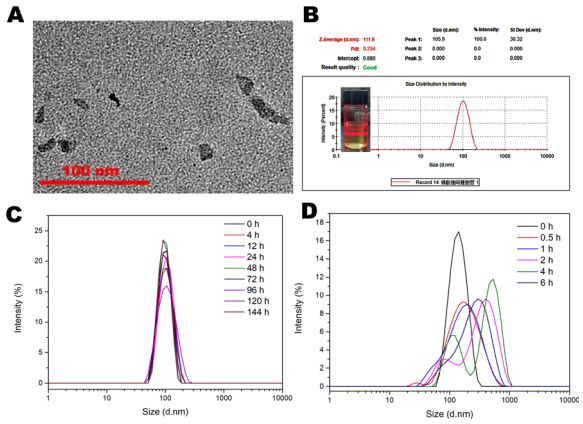

Fig. 3 Nanoparticle sizes of **GP-Ara-C** measured through (A) TEM and (B) DLS, (C) their stability in pH 7.4 PBS for 6 days and (D) their pH-responsive disruption in pH 6.0 PBS in 6 hours.

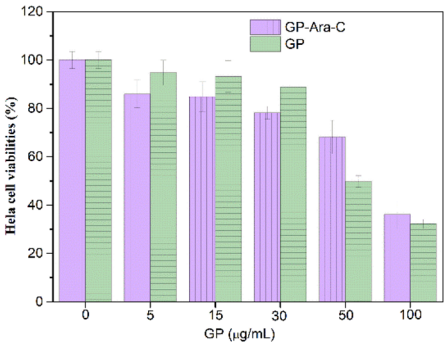

Fig. 4 HeLa cell viabilities of acetate GP and GP-Ara-C with different concentrations of GP at 24 h.

acetate **GP** and **GP-Ara-C** from the 96-well plate used in the CCK-8 assays. The morphology of the HeLa cells showed that the intact cell membranes were damaged, and numerous intact cells were significantly decreased in a drug concentration-dependent mode (Fig. 5).

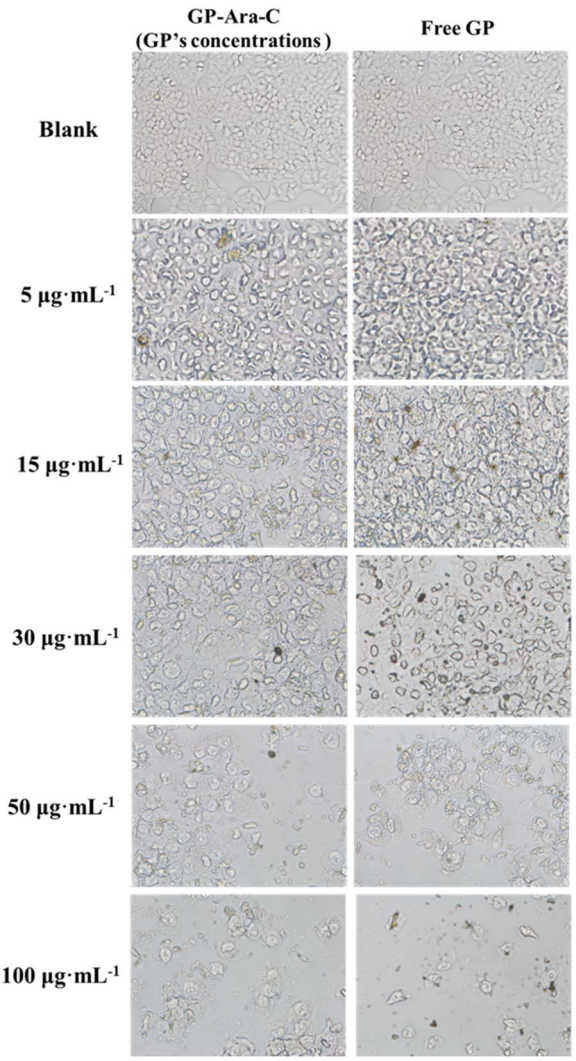

Fig. 5 Morphology of HeLa cells treated with different concentrations of acetate GP and GP-Ara-C (GP's concentration) from the 96-well plate in CCK-8 assays at 24 h.

Cellular uptake

To monitor the distribution of **GP-Ara-C** in HeLa cells, we prepared the DID encapsulated **GP-Ara-C** to observe the distribution of **GP-Ara-C**. Meanwhile, the free DID (red fluorescent probe) was used as the control group. We clearly observe that the free DID is completely distributed into the cell nuclei (blue color) in the merged image at 7 h. The blue color was not completely overlapped by red color (DID@**GP-Ara-C**) at 7 h (Fig. 6). These results confirmed that the assembled **GP-Ara-C** could affect the distribution of free DID in cells, meaning that the red color (DID fluorescent probe in **GP-Ara-C**) authentically delegated the position of assembled **GP-Ara-C** in cells. These results confirmed that the pathways of endocytosis were different between free DID and DID@**GP-Ara-C**. The authentic

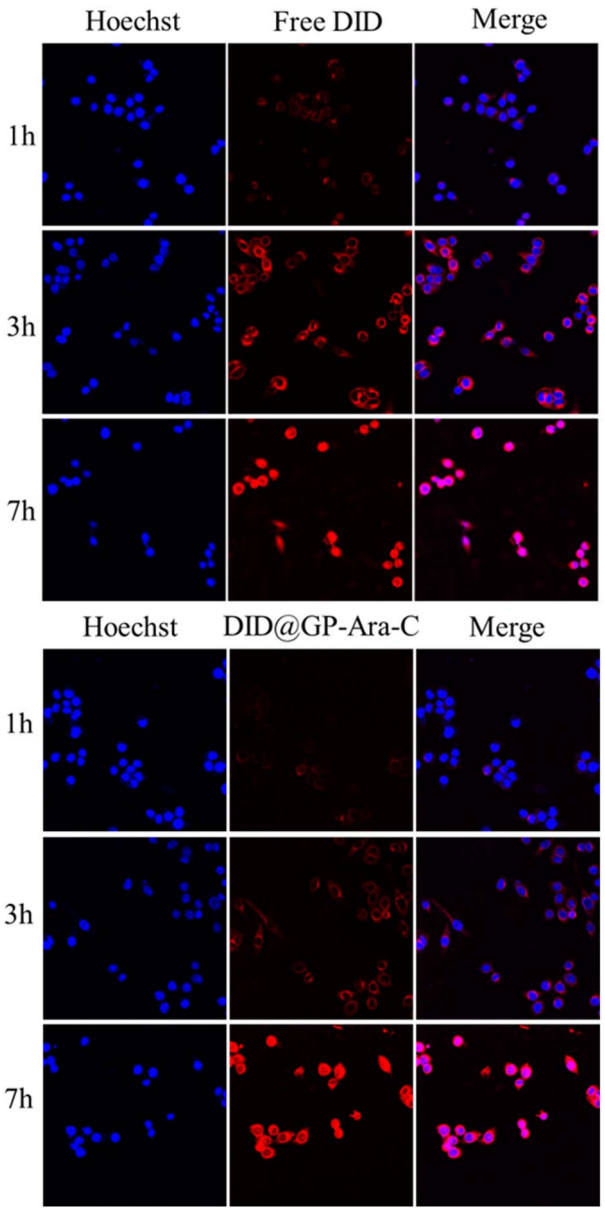

Fig. 6 Distribution of DID@GP-Ara-C in HeLa cells for 1 h, 3 h and 7 h monitored by CLSM (scale: 20×).

pathways of assembled **GP-Ara-C** could probably be clathrin-coated pit-mediated endocytosis (CME)[28] because the features of the HeLa cell and particle size of **GP-Ara-C** (100 nm) were consistent with the classical size of the endocytic vesicle phenomenon.[28] The different mechanisms of CME of **GP-Ara-C** and simple diffusion of DID probably could explain the different distribution of cell viability between free DID (or free **GP**) and **GP-Ara-C**.

Conclusions

In this study, we prepared a pH-responsive amphiphilic **GP-Ara-C** nanomedicine based on **GP** and **Ara-C**. The FT-IR, UV-vis, HPLC, TLC and MS results confirmed that the product of **GP-Ara-C** was successfully synthesized and purified. The TEM and DLS results demonstrated that assembled **GP-Ara-C** could be stable in pH 7.4 PBS for 6 days and disrupted in pH 6.0 PBS for hours. The cell viabilities showed that the anticancer abilities of free **GP** and **GP-Ara-C** were similar. Furthermore, **GP-Ara-C** was observed in the HeLa cell nuclei at 7 h in the cellular uptake experiment. Briefly, this simple and effective pH-responsive amphiphilic **GP-Ara-C** nanomedicine is a candidate for cancer therapy in clinics.

Data availability

The data supporting this article have been included as part of the ESI.†

Author contributions

Conceptualization: Ling-na Han and Xiao Duan; Data collection and analysis: Jianzhong Li, Qiang Wang, Hailong Liu, and Xinping Liu; funding acquisition: Xiao Duan and Ling-na Han; supervision: Xiao Duan; writing, review & editing: Jiangzhong Li, Xiao Duan and Ling-na Han.

Conflicts of interest

The authors declare no conflict of interest.

Acknowledgements

This work was supported by the National Natural Science Foundation of China (No. 82204327), the Research Project Supported by Shanxi Scholarship Council of China (No. 2024-136), the Program of Scientific and Technological Activities for Returned Scholars in Shanxi Province (No. 20230043), and the Scientific and Technological Innovation Programs of Higher Education Institutions in Shanxi, China (No. 2019L0676).

Notes and references

1 S. Li, M. Jiang, L. Wang and S. Yu, *Biomed. Pharmacother.*, 2020, **129**, 110389.
2 X. Pei, Z. Zhu, Z. Gan, J. Chen, X. Zhang, X. Cheng, Q. Wan and J. Wang, *Sci. Rep.*, 2020, **10**, 2717.
3 Z. Zhang, Y. Yue, L. Xu, Y. Wang, W. Geng, J. Li, X. Kong, X. Zhao, Y. Zheng, Y. Zhao, L. Shi, D. Guo and Y. Liu, *Adv. Mater.*, 2021, **33**, 2007719.
4 J. Chen, Y. Zhang, Z. Meng, L. Guo, X. Yuan, Y. Zhang, Y. Chai, J. L. Sessler, Q. Meng and C. Li, *Chem. Sci.*, 2020, **11**, 6275–6282.
5 M. Hu, P. Huang, Y. Wang, Y. Su, L. Zhou, X. Zhu and D. Yan, *Bioconjugate Chem.*, 2015, **26**(12), 2497–2506.
6 J. Zuo, X. Gao, J. Xiao and Y. Cheng, *Chin. Chem. Lett.*, 2023, **34**, 107827.
7 M. Sun, Q. Qian, L. Shi, L. Xu, Q. Liu, L. Zhou, X. Zhu, J. Yue and D. Yan, *Sci. China:Chem.*, 2020, **63**, 35–41.
8 H. Qu, L. Li, H. Chen, M. Tang, W. Cheng, T. Lin, L. Li, B. Li and X. Xue, *J. Controlled Release*, 2023, **363**, 361–375.
9 Y. Bai, C. Liu, J. Yang, C. Liu, Q. Shang and W. Tian, *Colloids Surf., B*, 2022, **217**, 112606.
10 J. Xi and H. Liu, *Adv. Ther.*, 2020, **3**, 1900107.
11 J. Xiang, X. Liu, G. Yuan, R. Zhang, Q. Zhou, T. Xie and Y. Shen, *Adv. Drug Delivery Rev.*, 2021, **179**, 114027.
12 P. Huang, D. Wang, Y. Su, W. Huang, Y. Zhou, D. Cui, X. Zhu and D. Yan, *J. Am. Chem. Soc.*, 2014, **136**(33), 11748–11756.
13 S. Dong, J. He, Y. Sun, D. Li, L. Li, M. Zhang and P. Ni, *Mol. Pharm.*, 2019, **16**(9), 3770–3779.
14 Q. Mou, Y. Ma, X. Zhu and D. Yan, *J. Controlled Release*, 2016, **238**(28), 34–44.
15 Y. Huang, L. Wang, H. Chang, W. Ye, M. K. Dowd, P. J. Wan and Y. C. Lin, *Anticancer Res.*, 2006, **26**(3A), 1925–1933.
16 H. Cao, K. Sethumadhavan, F. Cao and T. T. Y. Wang, *Sci. Rep.*, 2021, **11**, 5922.
17 J. Jiang, V. Slivova, A. Jedinak and D. Sliva, *Clin. Exp. Metastasis*, 2012, **29**, 165–178.
18 R. C. Stein, A. E. A. Joseph, S. A. Matlin, D. C. Cunningham, H. T. Ford and R. Charles Coombes, *Cancer Chemother. Pharmacol.*, 1992, **30**, 480–482.
19 J. Xiong, J. Li, Q. Yang, J. Wang, T. Su and S. Zhou, *Breast Cancer Res.*, 2017, **19**, 27.
20 Y. Liu, L. Wang, L. Zhao and Y. Zhang, *Nat. Prod. Rep.*, 2022, **39**, 1282.
21 J. Song, J. Yu, L. S. Jeong and S. K. Lee, *Cancer Lett.*, 2021, **497**, 54–65.
22 L. Hruba, V. Das, M. Hajduch and P. Dzubak, *Biochem. Pharmacol.*, 2023, **215**, 115741.
23 B. Marciniak, G. Schroeder, H. Kozubek and B. Brzezinski, *J. Chem. Soc., Perkin Trans. 1*, 1991, **2**, 1359–1362.
24 B. Brzezinski, J. Olejnik, S. Paszyc and T. F. Aripov, *J. Mol. Struct.*, 1990, **220**, 261–268.
25 L. Wang, Y. Liu, Y. Zhang, A. Yasin and L. Zhang, *Molecules*, 2019, **24**, 1286.
26 V. T. Dao, C. Gaspard, M. Mayer, G. H. Werner, S. N. Nguyen and R. J. Michelot, *Eur. J. Med. Chem.*, 2000, **35**, 805–813.
27 E. Matamoros, P. Cintas and J. C. Palacios, *Org. Biomol. Chem.*, 2019, **17**, 6229–6250.
28 J. J. Rennick, A. P. R. Johnston and R. G. Parton, *Nat. Nanotechnol.*, 2021, **16**, 266–276.